IRIS AperTO

UNIVERSITÀ DEGLI STUDI DI TORINO

AperTO - Archivio Istituzionale Open Access dell'Università di Torino

AKI recovery induced by mesenchymal stromal cell- derived extracellular vesicles carrying microrna

This is the author's manuscript

Original Citation:

Availability:

This version is available http://hdl.handle.net/2318/1531803 since 2016-08-12T10:51:00Z

Published version:

DOI:10.1681/ASN.2014070710

Terms of use:

Open Access

Anyone can freely access the full text of works made available as "Open Access". Works made available under a Creative Commons license can be used according to the terms and conditions of said license. Use of all other works requires consent of the right holder (author or publisher) if not exempted from copyright protection by the applicable law.

(Article begins on next page)

04 May 2023

Acute kidney injury recovery induced by extracellular vesicles carrying miRNAs

Federica Collino*[1,4], Stefania Bruno*[2], Danny Incarnato[3], Daniela Dettori[2,3], Francesco Neri[3], Paolo Provero[2,4], Margherita Pomatto[1], Salvatore Oliviero[3], Ciro Tetta[5], Peter Quesenberry[6] and Giovanni Camussi[1,#].

[1] Department of Medical Sciences,[2] Department of Molecular Biotechnology and Healthy Sciences, [3] Department of Life Sciences and System Biology and HUGEF, University of Torino,[4] Translational Center of Regenerative Medicine Unito/EMEA LA Medical Board, Fresenius Medical Care, Torino, Italy; [5] Center for Translational Genomics and Bioinformatics, San Raffaele Scientific Institute, Milan, Italy; [6] Department of Medicine, the Warren Alpert Medical School of Brown University, Providence, RI, USA.

* These authors contributed equally to this work.

Running title: mesenchymal stromal cell-derived extracellular vesicles and AKI recovery

Word Count

Abstract: 250

Text: 3029

 # Corresponding author:

Dr. G. Camussi, Dipartimento di Scienze Mediche, Ospedale Maggiore S. Giovanni Battista, Corso Dogliotti 14, 10126, Torino, Italy;

Phone +39-011-6336708, Fax +39-011-6631184.

E-mail: giovanni.camussi@unito.it

Abstract

Phenotypic changes induced by extracellular vesicles (EVs) have been implicated in recovery of acute kidney injury (AKI) induced by mesenchymal stromal cells (MSCs). microRNAs are potential candidates for cell reprogramming towards a pro-regenerative phenotype. The aim of the present study was to evaluate whether microRNA de-regulation inhibits the regenerative potential of MSCs and derived-EVs in a model of glycerol-induced AKI in SCID mice. For this purpose, we generated MSCs depleted of Drosha, a critical enzyme of miRNA maturation, to alter miRNA expression within MSCs and EVs. Drosha knock-down MSCs (MSC-Dsh) maintained the phenotype and differentiation capacity. They produced EVs that did not differ from those of wild type cells in quantity, surface molecule expression and internalization within renal tubular epithelial cells. However, EVs derived from MSC-Dsh (EV-Dsh) showed global down-regulation of miRNAs. Whereas, wild type MSCs and derived EVs were able to induce morphological and functional recovery in AKI, MSC-Dsh and EV-Dsh were ineffective. RNA sequencing analysis showed that genes deregulated in kidney of AKI mice were restored by treatment with MSCs and EVs but not by MSC-Dsh and EV-Dsh. Gene Ontology analysis showed that down-regulated genes in AKI were associated with fatty acid metabolism. The up-regulated genes in AKI were involved in inflammation, ECM-receptor interaction and cell adhesion molecules. These alterations were reverted by treatment with wild type MSCs and EVs, but not by the Drosha counterparts. In conclusion, miRNA depletion in MSCs and EVs significantly reduced their intrinsic regenerative potential in AKI, suggesting a critical role of miRNAs**.**

Introduction

Several studies demonstrated that mesenchymal stromal cells (MSCs) may promote recovery from acute kidney injury (AKI). The mechanism has been ascribed mainly to a paracrine action of MSC-derived mediators[1]. Bi et al.[2] demonstrated that the conditioned medium of MSCs mimics the therapeutic effects of the cells. We found that extracellular vesicles (EVs) released from MSCs contribute to their regenerative properties in glycerol induced AKI in SCID mice[3]. The regenerative potential of MSC-derived EVs has been described in several models of acute and chronic kidney injury[4, 5].

The mechanism of action of EVs has been attributed to the transfer of information between cells [6]. After internalization, EVs may deliver their proteins, lipid or nucleic acid content to recipient cells, changing their fate[7-9]. EVs released by MSCs were shown to express proteins involved in MSC self-renewal and differentiation capability[10]. Moreover, analysis of the nucleic acid composition of MSC-derived EVs demonstrated the presence of MSC specific mRNA and mature miRNAs[3, 11]. Recently, extracellular RNAs have been implicated both as promising biomarkers for a variety of pathologies[12, 13] and as mediators of several biological processes[14]. EVs represent a mechanism for the delivery of the nucleic acids in a degrading enzyme protective way[15]. The transfer of genetic information among cells is emerging as a new paradigm of cell to cell communication[16].

MicroRNAs (miRNAs)[17]are a class of small non-coding RNAs, abundant in the cell, that function as endogenous mediators of RNA silencing. miRNAs regulate protein expression by blocking both the mRNA transcription or the protein translation [18]. Two crucial enzymes play a relevant role in the regulation of miRNA maturation inside the cells, the RNase III Drosha and Dicer enzymes. The first one, acts in the nucleus where it cleaves the inactive pri-miRNA into the precursor miRNA (pre-miRNA), a double-stranded hairpin structure of about 70 nucleotides [19]. The pre-miRNA is then exported from the nucleus to the cytoplasm to finally generate a functional mature miRNA by Dicer

cleavage[20]. EV mediated transfer of functional miRNAs have been shown to occur in several contexts[21-23].

Whether EV-mediated transfer of miRNAs is implicated in the healing properties of MSC-derived vesicles in AKI has not yet been investigated. To address this issue, we evaluated the effect of the global suppression of miRNA biogenesis [24] by generation of Drosha knock-down MSCs to be used as EV donors. The choice of Drosha as target enzyme, was based on the knowledge that Drosha activity is restricted to the generation of miRNAs, whereas Dicer is involved in the biogenesis of multiple classes of small RNAs including siRNA [25-27]. Here, we reported that depletion of Drosha in MSCs, generated EVs with a deregulation of their miRNA content and altered the intrinsic regenerative potential of MSCs and their derived EVs. These data support the relevance of miRNAs shuttled by EVs in the healing properties of MSCs.

Results

Generation of Drosha knock-down MSCs

miRNA reduction was obtained by MSC transduction with a lentiviral, tetracycline inducible vector, containing a short hairpin RNA (shRNA) targeting Drosha (MSC-Dsh) and the red fluorescence protein (RFP). Transduced MSCs maintained the classical mesenchymal markers on their surface (Fig. 1A) as detected by FACS analysis and conserved their ability to differentiate in chondrocytes, adipocytes and osteocytes (not shown). To quantify the knock-down of Drosha, we performed quantitative real time (qRT)-PCR on Dsh-transduced MSCs, cultured with doxycycline in comparison with control transduced cells (MSC-CTRL). In cell populations from three separate donors, we observed a two-fold reduction ($p<0.01$) of Drosha transcript level (Fig. 1B) in MSC-Dsh in respect to MSC-CTRL. This reduction was enhanced in sorted RFP-positive MSC-Dsh (Fig. 1B, $p<0.01$). In all experiments, sorted MSC-CTRL and MSC-Dsh were used.

Characterization of EVs released from MSC-Dsh

EVs from MSC-Dsh (EV-Dsh) showed a size distribution comparable to the one released by MSC-CTRL (EV-CTRL) with a mean diameter of 128 ±19 and 130±19 nm, respectively (detected by Nanosight instrument). Cytofluorimetric analyses of EV-CTRL and EV-Dsh, showed the expression by EVs of antigens characteristic of the cells of origin, such as CD29, CD44, CD105, CD73, CD90 and HLA class I (Fig. 2A). EV-CTRL and EV-Dsh ($3x10^9$part/ml) were equally incorporated by murine tubular epithelial cells (mTEC), as observed by confocal microscopy after 24 hours of incubation (Fig. 2B). SYTO-RNA carried by EVs was transferred to target cells (Fig. 2B).

miRNA profile in EV-Dsh

miRNA screening and comparison in EV-Dsh and –CTRL was evaluated by qRT-PCR. Using a cut-off <35 Ct value in miRNA expression, we found 161 miRNAs detected in all the EV-CTRL samples

(n=4). Comparing the miRNA content between EV-CTRL and EV-Dsh, a global tendency to down-regulation of miRNAs in EV-Dsh in respect to EV-CTRL was observed (55±15% of all the expressed miRNAs). The intersection of the list of miRNAs down-regulated in different EV-Dsh in respect to EV-CTRL, identified 49 miRNAs, commonly down-regulated in EV-Dsh (Table 1, $p< 0,05$).

Impaired protective effect of MSC-Dsh in a model of glycerol-induced AKI

At day 3 after AKI induction, 75,000 MSC-CTRL or MSC-Dsh were administered intravenously. Mice were then sacrificed after 5 days from the induction of AKI. The lesions observed in AKI mice included tubular hyaline casts, vacuolization, and presence of necrosis of proximal and distal tubular epithelium (Fig. 3A). Morphological damage correlated with the significant rise in blood urea nitrogen (BUN, Fig. 3D). Injection of MSC-CTRL resulted in decrease of tubular lesions and evidence of renal tubular repair in respect to AKI mice treated with vehicle alone (Fig. 3B), in parallel with the reduction of BUN levels (Fig. 3D). On the contrary, injection of MSC-Dsh did not significantly improve morphological (Fig. 3C) or functional injury (Fig. 3D). The quantitative evaluation of casts (Fig. 3E) and tubular necrosis (Fig. 3F) showed a significant reduction in MSC-CTRL but not in MSC-Dsh treated mice.

We also compared the effect of EVs from MSC-Dsh (EV-Dsh) with that of EVs derived from wild type MSCs (EV-CTRL). For this purpose, we injected $2.2x10^8$ particles/mice of EV-CTRL and EV-Dsh at day 3, after AKI induction. In mice treated with EV-CTRL but not with EV-Dsh, the tubular lesions at day 5 were significantly less severe than in untreated AKI mice (Fig. 4A-C). In control healthy mice, injected with EV-CTRL and EV-Dsh, the histological analysis and BUN measurement demonstrated no negative effects associated with the EV-CTRL and EV-Dsh injection (Fig. 4 D-G), in the absence of AKI damage. EV-Dsh injection in AKI mice didn't inhibit the rise of BUN (Fig. 4G). Also the counts of hyaline casts and tubular necrosis, demonstrated the inefficiency of EV-Dsh in respect to the EV-CTRL (Fig. 4 H and I).

MSC-CTRL but not MSC-Dsh induced a pro-regenerative gene signature in the kidney

In order to detect the molecular changes occurred in the kidneys of treated animals, we performed RNA-Seq analysis (GEO number, GSE59958). We observed a strong correlation between MSC-CTRL and EV-CTRL treated mice (Pearson Correlation Coefficient, PCC 0.96). Interestingly, comparison of MSC-CTRL and EV-CTRL treatment with the AKI condition showed a lower degree of correlation (PCC 0.72 and 0.74, respectively), indicating that both treatments partially reverted the molecular changes occurring in the kidney after glycerol-induced damage. Moreover, this was confirmed by the observation that healthy mice significantly correlated with MSC-CTRL and EV-CTRL samples (PCC 0.966 and 0.858, respectively, Fig. 5A). On the contrary, transcriptome profile of MSC-Dsh and EV-Dsh treated mice showed a high correlation with the untreated AKI mice (PCC 0.997 and 0.988, respectively), and low or no correlation with the healthy samples (PCC 0.486 and 0.384, respectively), indicating no healing properties associated with Drosha knock-down MSC or EV-Dsh treatments (Fig. 5A).

Consistently, differential expression analysis of all the genes de-regulated in AKI versus healthy kidney samples (*n=2663*, up-regulated; *n=1893*, down-regulated), showed an extremely similar pattern (Fig. 5B). The EV-CTRL and MSC-CTRL were clustered into two major groups supporting a relevant overlap in the genes regulated by both cells and EVs during AKI repair (Fig. 5B). Interestingly, MSC-Dsh and EV-Dsh kidneys showed a global gene expression pattern very similar to that of AKI (Fig. 5B). These results suggested that MSCs depleted of Dsh were unable to activate the pro-regenerative transcriptomic program in injured kidneys. In fact, genes altered in AKI vs. healthy condition, showed a significant reversion to physiological levels in EV-CTRL and MSC-CTRL treatments, compared to EV-Dsh and MSC-Dsh treatments (EV-CTRL vs EV-Dsh, $p= 2.3\ e^{-142}$ and $6.8\ e^{-46}$ for up-regulated and down-regulated genes respectively; MSC-CTRL vs MSC-Dsh, $p= 1.2\ e^{-307}$ and $3.0\ e^{-84}$ for up-regulated and down-regulated genes respectively) (Fig. 5C).

Gene ontology analysis

Focusing on genes with a significant fold change among all the treatments (FC >= |1|), we detected a relevant group of transcripts significant reverted after MSC-CTRL (*n=702 and 428,* respectively down- and up-regulated in respect to AKI, Fig. 6A) and EV-CTRL stimulation (*n= 610 and 706,* respectively down- and up-regulated in respect to AKI, Fig. 6B). The same modulation was not observed for the –Dsh treatments (*n= 33 and 77* for MSC-Dsh and *n= 111 and 129* for EV-Dsh, respectively up- and down- in respect to AKI, Fig. 6A, B).

Gene Ontology analysis (GO) was performed on a subset of genes that showed comparable high modulation in both MSC and EV treatments. This yield final subsets of 335 and 325 respectively up- and down-regulated genes common to MSC- and EV-CTRL treatments with respect to AKI (Fig. 6C), or 225 and 110 respectively up- and down-regulated genes common to MSC- and EV-CTRL treatments with respect to –Dsh (Fig. 6D). The GO enrichment analysis revealed that common up-regulated transcripts in EV- and MSC-CTRL in respect to AKI, were enriched for genes associated with the regulation of metabolic pathways (Valine, leucine and isoleucine degradation; Tryptophan and Butanoate metabolism, PPAR signaling pathway, p= $2{,}36E^{-09}$, $1{,}74E^{-06}$ and $4{,}71E^{-05}$ respectively) but also for genes involved in the complement and coagulation cascades (Fig. 6E, p= 1,00E-04). The most representative GO of the down-regulated genes was associated with response to inflammation, ECM-receptor interaction, cell adhesion molecules and cell cycle (Fig. 6F, p= $1{,}60E^{-04}$, $1{,}05E^{-06}$, $1{,}56E^{-02}$ and $4{,}11E^{-02}$ respectively). Cross-match of the common genes modulated after MSC- or EV-Dsh treatments in respect to AKI showed no significant enrichment of these pathways (not shown). Genes co-modulated in EV- and MSC-CTRL in respect to –Dsh were associated to :ECM-remodeling and focal adhesion (for the down-regulated transcripts) and metabolic regulation (for the up-regulated transcripts) (Supplementary Table 1).

miRNA:mRNA data integration

To identify potential mRNA targets for vesicle-carried miRNAs, we first clustered the miRNAs expressed in EV-CTRL (n=161) into families, according to their seed sequence, and scanned the 3'-UTR of AKI-expressed genes for perfect seed-match occurrences (6-8mers). Moreover, to account for potential cooperative action of different miRNAs, we restricted our research to those genes targeted by at least 2 expressed miRNA families. Our analysis produced a list of 16 significantly enriched miRNA families ($p < 0.05$, Hypergeometric distribution), associated in 15 pairs, whose targets show significant down-regulation in EV-CTRL versus AKI mice (Supplementary Table 2). For 8 of these miRNA families, at least one representative miRNA was differentially expressed in EV–Dsh, supporting their involvement in the EV healing process. In particular, we found a significant enrichment for miR-483-5p, miR-191, miR-28-3p, miR-423-5p, miR-744, miR-129-3p, miR-24 and miR-148a families. The union of the targets for the 15 pairs of miRNA families, identified 209 genes potentially modulated by these miRNAs, of which 165 genes (77.8%) were not reverted in EV-Dsh treatment in respect to AKI. GO enrichment analysis of these targets showed the over-representation of processes associated with ECM-receptor interaction and focal adhesion ($p= 1{,}00E^{-04}$, $3{,}00E^{-03}$) and with Wnt and p53 pathways (Supplementary Table 3, $p= 1{,}90E^{-02}$ and $3{,}50E^{-02}$ respectively).

Effect of Drosha knock-down on the expression of markers of kidney injury

Kidneys from untreated AKI mice showed elevated levels of transcripts coding for markers of tubular damage such as lipocalin 2 (Lcn2) [28] and fibrinogen subunits (Fg) [29] as detected by RNA-Seq analysis. In healthy mice, no expression of Lcn2 was observed. The treatment with MSC- and EV-CTRL led to significant decrease of Lcn2 (Fig. 7A), while MSC- or EV-Dsh injected mice maintained elevated levels of Lcn2 transcript (Fig. 7A). Lcn2 down-regulation after both MSC-CTRL and EV-CTRL treatments, was confirmed by qRT-PCR (n=6 mice/group, Fig. 7B). MSC- and EV-Dhs injected animals maintained elevated levels of Lcn2 (Fig. 7B).

We also evaluated the levels of fibrinogen, as another important marker of AKI damage (29). AKI induced the up-regulation of all the Fg subunits (-α, –β and –γ) (Fig. 7C). MSC- or EV-CTRL treated mice showed the down-regulation of the Fg-β, but less relevant reduction of α and γ subunits. MSC- or EV-Dsh injected mice maintained elevated levels of all the Fg subunits (Fig. 7C-D). In healthy mice no or minimal expression of all the Fg-subunits was observed. qRT-PCR of whole kidney confirmed minimal expression of Fg-β in control kidneys (Fig. 7E). A robust increase of Fg-β was observed after 5 days in AKI-untreated as well as in mice treated with MSC-Dsh and EV-Dsh. MSC-CTRL and EV-CTRL reverted the Fg-β expression showing transcript expression comparable to that of healthy mice (Fig. 7E). Healthy mice injected with EV-CTRL and EV-Dsh showed levels of expression of Lcn2 and Fg-β, comparable to that of healthy untreated animals (not shown). These data collectively indicated that injured renal tubules can initiate local fibrinogen synthesis [29]. Immunohistochemistry analysis of Fg-β in untreated AKI mice, showed a strong peritubular staining for fibrinogen and some positivity in the tubular cell cytoplasm (Fig. 7F). Tubular staining was not observed in kidneys from healthy mice and was markedly reduced in mice treated with MSC- and EV-CTRL but not –Dsh (Fig. 7F).

Discussion

The results of the present study demonstrated that the down-regulation of miRNAs in human MSCs, reduced the intrinsic kidney pro-regenerative properties of these cells and of their derived-EVs. This effect was associated with changes in miRNA composition of cells and EVs. Previous studies demonstrated that EVs derived from human MSCs were able to favor recovery of AKI by activation of anti-apoptotic and pro-regenerative programs in tubular epithelial cells[3, 30, 31, 32]. Transfer of mRNAs from MSCs to tubular epithelial cells was observed both *in vitro* and *in vivo* [3]. The mRNA transfer, observed also in other models[33,34], was shown to be followed by their transient transduction into proteins. We recently demonstrated an EV-mediated transfer of miRNAs from MSCs to tubular epithelial cells in an *in vitro* model of renal tubular cell injury induced by ATP depletion[35]. miRNA modulation in renal tubular cells, was associated with functional recovery and phenotypic changes[36]. In the present study, we evaluated whether EV-shuttled miRNAs play a critical role in the healing properties of MSCs in an *in vivo* model of AKI induced by glycerol administration. We observed that knock-down of Drosha in MSCs, globally reduced miRNA content in the EVs. Moreover, MSC and EV-Dsh exhibited a significantly reduced pro-regenerative effect in AKI mice in respect to the wild type MSCs and EVs. The lack of EV-Dsh efficacy was not dependent on reduced internalization or expression of surface molecules but rather to the molecular content of EVs. The efficacy of wild type MSCs and EVs in the recovery from AKI was observed not only at functional and morphological but also at molecular level. Transcriptome analysis of the kidney from AKI mice showed the alteration of about 4.556 genes in respect to healthy mice. The genes down-regulated by AKI were associated with metabolism such as Valine, leucine and isoleucine degradation; Tryptophan and Butanoate and fatty acid metabolism. Different reports documented the importance of mitochondrial fatty acid oxidation (FAO) in the cytoprotection of proximal tubule cells during the development of AKI [36]. Among the genes positively modulated by wild type MSCs and EV treatment, the enrichment of genes acting in

metabolic pathways associated with fatty acid oxidation, glycolysis, gluconeogenesis and ketone bodies generation has been detected. These processes has been involved in the regulation of energy metabolism of damage tubular epithelial cells by MSC treatment[37].

Moreover, AKI damage was associated with the up-regulation of genes associated with inflammation, ECM-receptor interaction, cell adhesion molecules and cell cycle in respect to healthy controls. Treatment with wild type MSC and EVs restored a normal transcriptome pattern. In contrast, Dsh knock-down cells and EVs were unable to inhibit the molecular alteration observed in AKI and the RNA-Seq analysis showed a superimposable pattern between AKI and -Dsh treated mice. Recent studies correlated Lcn2 and Fg-β expression with AKI progress in mice [28, 29]. Over-expression of these markers of renal injury was reduced by wild type MSCs and EVs but not by MSC- and EV-Dsh. Inefficiency of Drosha knock-down cells and EVs in inducing renal repair was observed not only at morphological level but also at functional levels as indicated by the persistence of elevated BUN level. In the attempt to identify the possible healing miRNAs shuttled by EVs, we showed statistically significant correlation of 16 miRNA family (associated in 15 pairs) with genes, whose targets show significant down-regulation in EV-CTRL treated animals in respect to AKI. Of them, 8 miRNA families resulted significant reduced in EV-Dsh (miR-483-5p, miR-191, miR-28-3p, miR-423-5p, miR-744, miR-129-3p, miR-24 and miR-148a families). Union of genes of the 15 pairs of miRNAs identified 209 genes, potentially modulated by these miRNAs. GO enrichment analysis of these targets showed the over-representation of processes associated with the first stages of kidney damage and repair by stem cell administration such as the cell adhesion molecules (CAM) and MAPK signaling [38]. Interestingly, Wnt signaling pathway [39], ECM-remodeling [40] and p53 pathway [41] were also present among the significant biological process identified (not shown). These processes are usually associated to relevant stages in the transition from acute to chronic injury such as vascular failure, interstitial

fibrosis, and glomerulosclerosis development [38-41]. By selecting in this set, only genes not reverted in EV-Dsh treatment in respect to AKI, 165 genes resulted the possible miRNA targets. GO enrichment analysis of these genes showed that EV-Dsh treated mice overexpressed genes associated with processes related with the progression of kidney damage such as Wnt pathway, p53 signaling, ECM-remodeling and focal adhesion processes as the untreated AKI.

In conclusion, the results of the present study indicate that miRNAs play a critical role in the regenerative potential of MSCs. The global down-regulation of miRNAs obtained by Drosha knock-down in MSCs abrogated the ability to promote AKI recovery both by cells and EVs.

Concise methods

Culture of bone marrow MSC

Bone marrow cells were obtained by Lonza (Basel, Switzerland) and cultured as previously described (3). Cells were seeded at a density of 10,000 cells/cm^2 and used within the seven passage. Cytofluorimetric analysis was performed as described [3] and the following monoclonal antibodies conjugated with Allophycocyanin (APC) or Fluorescein (FITC), were used: anti-CD146, -CD44, -CD105, -CD29 and -CD90. Mouse IgG isotypic controls were from Miltenyi (Bergisch Gladbach, Germany). All of the cell preparations at different passages of culture expressed the typical MSC markers: CD105, CD73, CD44, CD90, CD166, and CD146. They also expressed HLA class I. The adipogenic and osteogenic differentiation ability of MSC was determined as previously described [3].

Transduction of MSC with lentiviral particles

Lentiviral particles were produced using the 3th generation core packing plasmids kindly provided by Dr. Calautti (Department of Molecular Biotechnology and Life Sciences, Torino). Virus particles were released by 293T cells after overnight collection, filtered through a 0.45 mm filter and concentrated by ultracentrifugation as previous described [42]. For the construct targeting Drosha, approximately 10^5 passage 0 hMSCs were transduced with particles containing the pTRIPZ lentiviral inducible vector shRNAmiR targeting Drosha (Open Biosystem, clone V2THS_71783) with a single infection. Transduction efficiency was determined by measuring the % of RFP positive cells using different doses of lentivirus. Wild type cells were transduced with a pTRIPZ lentiviral inducible vector scramble-shRNAmiR. Following transduction, cells were grown out to 70% confluence in complete medium containing doxycycline (1μg/ml). RFP-positive cells were selected using a MoFlo™ Cell Sorter (Dakocytomation, Copenhagen, Denmark). Sorted RFP$^+$ cells were characterized by incubation with FITC- or APC-conjugated antibodies. Ten thousand cells were analyzed at each experimental point.

Doxycycline was added to cultured cells every time they reached the semi-confluent stage and the medium was changed after 72 hours during the duration of the experiment to avoid fluctuation in the Drosha transcript level. Drosha expression was evaluated by quantitative real time PCR using the following primers: F1- 5-CATGCACCAGATTCTCCTGTA-3 and R1 5-GTCTCCTGCATAACTCAACTG-3 as previous described [43].

Isolation of EVs

EVs were obtained from supernatants of MSCs cultured in RPMI deprived of FCS, supplemented with 0.5% of BSA (Sigma) and in the presence of doxycycline. The viability of cells incubated overnight without serum was > 98% as detected by trypan blue exclusion. No apoptotic cells were detected by TUNEL assay. Supernatants of MSCs were first centrifuged at 300g and 10.000 g to remove debris, apoptotic bodies, large vesicles and then submitted to ultracentrifugation for 1 hours at 4°C at 100.000g (Beckman Coulter Optima L-90K ultracentrifuge; Beckman Coulter, Fullerton, CA) as previously described [44].

EV dimension and profile were analyzed by Nanosight LM10 (NanoSight Ltd, Minton Park, UK) and the protein content was quantified by Bradford (BioRad, Hercules, CA). Endotoxin contamination of EVs was excluded by Limulus testing according to the manufacturer's instruction (Charles River Laboratories, Inc., Wilmington, MA), and EVs were stored at −80 °C. To trace EVs by fluorescence microscopy, MSCs were labeled with the SYTO-RNA Select green fluorescent cell stain (Molecular Probes, Life Tecnhology) that specifically stain RNA, and with a lipophilic membrane stain that diffuses laterally to stain the entire cell (Life Tech) [45]. EVs obtained from labeled cells were washed by ultra-centrifugation as described below.

EV characterization

EVs were characterized by cytofluorimetric analysis using FITC or APC conjugated antibodies against CD73, CD44, CD105, CD90, CD29 and HLA-class I. FITC or APC mouse non-immune isotypic IgG

(Miltenyi Biotec,) were used as control. Briefly, EVs ($1.5x10^8$ particles) were incubated for 15 min at 4°C with antibodies then diluted in 1 to 3 and immediately acquired as described by as previously described [46]. FACS analysis was acquired using Guava easyCyte Flow Cytometer (Millipore, Billerica, MA, USA) and analyzed with InCyte software [46].

Isolation and culture of mTEC

Kidneys were obtained from healthy female C57 mice. mTEC were isolated, cultured and characterized for expression of tubular and negative for endothelial and glomerular markers as previously described by [3]. To determine the incorporation efficacy of EV-Dsh in respect to EV-CTRL by mTEC, we incubated EVs ($3x10^9$ part/ml) double-labeled with SYTO-RNASelect and Vybrant® Dil (both Molecular Probes) [45] with mTEC for 24 hours. The up-take of EVs was analyzed confocal microscopy (Zeiss LSM 5 Pascal, Carl Zeiss, Oberkochen, Germany).

RNA isolation and screening

Total RNA was isolated from cells and EVs using the mirVana RNA isolation kit (Applied Biosystem) according to the manufacturer's protocol. For the extraction of the RNA from kidneys Trizol reagent was used. RNA was then quantified spectrophotometrically (Nanodrop ND-1000, Wilmington DE) and the RNA quality was assessed by capillary electrophoresis on an Agilent 2100 Bioanalyzer (Agilent Technologies, Inc, Santa Clara, CA) using the Total Eukaryotic Nano and Small RNA kits.

RNA-Seq

For RNA-Seq library preparation, approximately 2 μg of total RNA from mouse kidney was subjected to poly(A) selection, and libraries were prepared using the TruSeq RNA Sample Prep Kit (Illumina) following the manufacturer's instructions. Sequencing was performed on the Illumina HiScanSQ platform. Reads were mapped to the *Mus musculus* mm9 reference assembly using TopHat v2.0.10 [47], and RPKM for transcripts were calculated with Cufflinks v2.1.1 [48]. Transcripts with RPKM ≥ 1 were

further considered for differential expression analysis. Genes with $\log_2(FC) \geq 1$ and $\log_2(FC) \leq -1$ were respectively considered as up- or down-regulated. Gene Ontology analysis was performed using DAVID Bioinformatics Resource [49].

RNA-Seq data have been deposited in the Gene Expression Omnibus (GEO number, GSE59958, http://www.ncbi.nlm.nih.gov/geo/query/acc.cgi?acc=GSE59958).

RNA and miRNA expression analysis.

RNA expression confirmation was conducted by real-time PCR (qRT-PCR). First-strand cDNA preparation and qRT-PCR experiments were performed as previous described [35]. qRT-PCR was performed using a 96-well StepOne™ Real Time System (Applied Biosystems) Fold change in mRNA expression was calculated as $2^{-\Delta\Delta}Ct$, using mGAPDH gene as normalizer. All the sequence-specific oligonucleotide primers were purchased from MWG-Biotech AG, Ebersberg, Germany (www.mwg-biotech.com).

To analyze the miRNA content in MSC and EV-CTRL and –Dsh, the Applied Biosystems TaqManH MicroRNA Assay Human Panel Early Access kit (Life Technologies) was used to profile 754 mature miRNAs by sequential steps of reverse transcription (Megaplex RT Pools; Life Technologies) using an Applied Biosystems 7900H qRT-PCR instrument. Raw Ct values, automatic baseline and threshold were calculate using the SDS software version 2.3. Comparison of miRNA expression was conducted using the Expression Suite software (Life Technologies). Fold change (Rq) in miRNA expression in EV-Dsh in respect to EV-CTRL was calculated as $2^{-\Delta\Delta Ct}$, using the RNU-48 as normalizer. Rq was measured for each sample and obtained comparing eight EV samples (*n=4/each group*). Statistical significance was set at $p<0.05$ and measured by *pair Student's t-test*. Only statistically reduced miRNAs in all samples tested would be considered for further studies.

miRNA target sites enrichment analysis

For miRNA target sites analysis, miRNAs expressed in EV-CTRL were clustered in families according to their seed sequence (nt 2-7). For each down-regulated gene with a fold-change of at least -1 in EV-CTRL vs. AKI mice , we extracted the 3'-UTR sequence, and performed a screening for perfect targets (6-8mers) for each miRNA family. For genes with multiple isoforms, only the isoform with the longest 3'-UTR was used. To account for potential miRNA cooperatively, we searched for targets enriched for seed-match sequences of at least 2 expressed miRNA families. The expected number of targets (used as background) for each pair of miRNA families was calculated on the whole Refseq annotation (21,164 genes). Statistical significance was assessed using an Hypergeometric test.

SCID Mice Model of AKI

Studies were approved by the Ethic Committee of Turin University and conducted in accordance with the National Institute of Health Guide for the Care and Use of Laboratory Animals. A model of rhabdomyolisis-induced acute kidney injury (AKI) was performed in male SCID mice as previous described [3]. On day 3 after glycerol administration, mice received an intravenous injection into the tail vein of 75.000 MSC-CTRL or MSC-Dsh cells; and EV-CTRL or EV-Dsh in 150 µl saline, or saline alone. The number of particles injected ($2.2x10^8$ particles/mice) corresponds to an average of the amount of EVs released overnight by 75.000 MSCs (average of 2.900 EVs/cell), which showed a therapeutic effect on this AKI model [3]. Mice were killed at day 5 (n =8 per group) after glycerol administration and blood samples for BUN determination and kidney specimens were collected. For gene expression, small pieces of the kidney cortical regions were stored in RNA later solution (Applied Biosystem) at -20 °C until required.

Statistical analysis

Data were analyzed using the GraphPad Prism 6.0 Demo program. Statistical analyses were conducted using One-way ANOVA with Newman-Keuls or Dunnett post-tests and *Student's t-test* where appropriated. Statistical significance was established at $p < 0.05$.

Acknowledgments:

Research reported in this publication was supported by the European Community Marie Curie Actions, IAPP2013_EVStemInjury Award number 612224 and by National Center For Advancing Translational Sciences of the National Institutes of Health under Award number UH2TR000880. The content is solely the responsibility of the authors and does not necessarily represent the official views of the National Institutes of Health.

We thank Federica Antico and Dr. Claudia Cavallari for technical help.

Statement of competing financial interests

C.T. and F.C. (Fresenius Medical Care) are employed by a commercial company and contributed to the study as researchers. C.T. and G.C. are named inventors in related patents.

References

1. Humphreys BD, Valerius MT, Kobayashi A, Mugford JW, Soeung S, Duffield JS, McMahon AP, Bonventre JV: Intrinsic epithelial cells repair the kidney after injury. *Cell Stem Cell* 2: 284-291, 2008. doi: 10.1016/j.stem.2008.01.014.

2. Bi B, Schmitt R, Israilova M, Nishio H, Cantley LG: Stromal cells protect against acute tubular injury via an endocrine effect. *J Am Soc Nephrol* 18:2486-2496, 2007.

3. Bruno S, Grange C, Deregibus MC, Calogero RA, Saviozzi S, Collino F, Morando L, Busca A, Falda M, Bussolati B, Tetta C, Camussi G: Mesenchymal stem cell-derived microvesicles protect against acute tubular injury. J Am Soc Nephrol 20:1053-1067, 2009.

4. Bruno S, Grange C, Collino F, Deregibus MC, Cantaluppi V, Biancone L, et al: Microvesicles derived from mesenchymal stem cells enhance survival in a lethal model of acute kidney injury. *PLoS One* 7:e33115, 2012.

5. He J, Wang Y, Sun S, Yu M, Wang C, Pei X, Zhu B, Wu J, Zhao W: Bone marrow stem cells-derived microvesicles protect against renal injury in the mouse remnant kidney model. *Nephrology* 17:493-500, 2012.

6. Akers JC, Gonda D, Kim R, Carter BS, Chen CC: Biogenesis of extracellular vesicles (EV): exosomes, microvesicles, retrovirus-like vesicles and apoptotic bodies. *J Neurooncol* 113:1-11, 2013.

7. Lee Y, El Andaloussi S, Wood MJ: Exosomes and microvesicles: extracellular vesicles for genetic information transfer and gene therapy. *Hum Mol Genet.* 2012, 21:R125-134.

8. Ratajczak J, Miekus K, Kucia M, Zhang J, Reca R, Dvorak P, Ratajczak MZ: Embryonic stem cell-derived microvesicles reprogram hematopoietic progenitors: evidence for horizontal transfer of mRNA and protein delivery. Leukemia. 2006. 20:847-856.

9. Aliotta JM, Pereira M, Amaral A, Sorokina A, Igbinoba Z, Hasslinger A, El-Bizri R, Rounds SI, Quesenberry PJ, Klinger JR: Induction of pulmonaryhypertensive changes by extracellular

vesicles from monocrotaline-treated mice. *Cardiovasc Res.* 2013 100:354-362. doi: 10.1093/cvr/cvt184.

10. Kim HS, Choi DY, Yun SJ, Choi SM, Kang JW, Jung JW, Hwang D, Kim KP, Kim DW: Proteomic analysis of microvesicles derived from human mesenchymal stem cells. J Proteome Res 11:839-849, 2012.

11. Collino F, Deregibus MC, Bruno S, Sterpone L, Aghemo G, Viltono L, Tetta C, Camussi G: Microvesicles derived from adult human bone marrow and tissue specific mesenchymal stem cells shuttle selected pattern of miRNAs. *PLoS One* 5:e11803, 2010.

12. Maluf DG, Dumur CI, Suh JL, Scian MJ, King AL, Cathro H, Lee JK, Gehrau RC, Brayman KL, Gallon L, Mas VR: The urine microRNA profile may help monitor post-transplant renal graft function. *Kidney Int.* 85:439-449, 2014.

13. Kong YW, Ferland-McCollough D, Jackson TJ, Bushell M: microRNAs in cancer management. *Lancet Oncol.* 13: e249-258, 2012. doi:10.1016/S1470-2045(12)70073-6.

14. Blelloch R, Gutkind JS: Epigenetics, noncoding RNAs, and cell signaling--crossroads in the regulation of cell fate decisions. *Curr Opin Cell Biol*, 25:149-151, 2013. doi: 10.1016/j.ceb.2013.02.019.

15. Arroyo JD, Chevillet JR, Kroh EM, Ruf IK, Pritchard CC, Gibson DF, Mitchell PS, Bennett CF, Pogosova-Agadjanyan EL, Stirewalt DL, Tait JF, Tewari M: Argonaute2 complexes carry a population of circulating microRNAs independent of vesicles in human plasma. *Proc Natl Acad Sci U S A*, 108:5003-5008, 2011. doi: 10.1073/pnas.1019055108.

16. Quesenberry PJ, Goldberg LR, Aliotta JM, Dooner MS, Pereira MG, Wen S, Camussi G. Cellular phenotype and extracellular vesicles: basic and clinical considerations. *Stem Cells Dev.* 2014; 23: 1429-1436.

17. Cech TR, Steitz JA: The noncoding RNA revolution-trashing old rules to forge new ones. *Cell,* 157: 77-94, 2014. doi: 10.1016/j.cell.2014.03.008.

18. Bartel DP: MicroRNAs: target recognition and regulatory functions. *Cell* 136: 215-233, 2009.

19. Han J, Lee Y, Yeom KH, Kim YK, Jin H, Kim VN: The Drosha-DGCR8 complex in primary microRNA processing. *Genes Dev* 18: 3016-3027, 2004.

20. Leisegang MS, Martin R, Ramírez AS, Bohnsack MT: Exportin t and Exportin 5: tRNA and miRNA biogenesis -and beyond. *Biol Chem*. 393:599-604, 2012. doi: 10.1515/hsz-2012-0146.

21. Valadi H, Ekström K, Bossios A, Sjöstrand M, Lee JJ, Lötvall JO: Exosome-mediated transfer of mRNAs and microRNAs is a novel mechanism of genetic exchange between cells. *Nat Cell Biol*.; 9: 654-659, 2007.

22. Yuan A, Farber EL, Rapoport AL, Tejada D, Deniskin R, Akhmedov NB, Farber DB: Transfer of microRNAs by embryonic stem cell microvesicles. *PLoS One*, 4: e4722, 2009.

23. Xin H, Li Y, Buller B, Katakowski M, Zhang Y, Wang X, et al. Exosome-mediated transfer of miR-133b from multipotent mesenchymal stromal cells to neural cells contributes to neurite outgrowth. *Stem Cells.* 30: 1556-1564, 2012.

24. Jinek M, Doudna JA: A three-dimensional view of the molecular machinery of RNA interference. *Nature.* 457:405-412, 2009. doi: 10.1038/nature07755.

25. Merritt WM, Bar-Eli M, Sood AK: The dicey role of Dicer: implications for RNAi therapy. *Cancer Res.*, 70. 2571-2574, 2010. doi: 10.1158/0008-5472.CAN-09-2536.

26. Volk N, Shomron N: Versatility of MicroRNA biogenesis. *PLoS One* 6: e19391, 2011. doi: 10.1371/journal.pone.0019391.

27. Xie M, Steitz JA: Versatile microRNA biogenesis in animals and their viruses. *RNA Biol.* 11, 2014. [Epub ahead of print].

28. Kashiwagi E, Tonomura Y, Kondo C, Masuno K, Fujisawa K, Tsuchiya N, Matsushima S, Torii M, Takasu N, Izawa T, Kuwamura M, Yamate J: Involvement of neutrophil gelatinase-associated lipocalin and osteopontin in renal tubular regeneration and interstitial fibrosis after cisplatin-induced renal failure. *Exp Toxicol Pathol.* 66: 301-311, 2014.

29. Sörensen-Zender I, Rong S, Susnik N, Lange J, Gueler F, Degen JL, Melk A, Haller H, Schmitt R: Role of fibrinogen in acute ischemic kidney injury. *Am J Physiol Renal Physiol*. 305:F777-785, 2013. doi: 10.1152/ajprenal.00418.2012.

30. Qi S, Wu D: Bone marrow-derived mesenchymal stem cells protect against cisplatin-induced acute kidney injury in rats by inhibiting cell apoptosis. *Int J Mol Med.* 32:1262-272, 2013. doi: 10.3892/ijmm.2013.1517.

31. Kim JH, Park DJ, Yun JC, Jung MH, Yeo HD, Kim HJ, Kim DW, Yang JI, Lee GW, Jeong SH, Roh GS, Chang SH: Human adipose tissue-derived mesenchymal stem cells protect kidneys from cisplatin nephrotoxicity in rats. *Am J Physiol Renal Physiol.* 302: F1141-1150, 2012.

32. Zhou Y, Xu H, Xu W, Wang B, Wu H, Tao Y, Zhang B, Wang M, Mao F, Yan Y, Gao S, Gu H, Zhu W, Qian H: Exosomes released by human umbilical cord mesenchymal stem cells protect against cisplatin-induced renal oxidative stress and apoptosis in vivo and in vitro. *Stem Cell Res Ther*. 2013;4: 34.

33. Del Tatto M, Ng T, Aliotta JM, Colvin GA, Dooner MS, Berz D, Dooner GJ, Papa EF, Hixson DC, Ramratnam B, Aswad BI, Sears EH, Reagan J, Quesenberry PJ: Marrow cell genetic phenotype change induced by human lung cancer cells. *Exp Hematol.* 39:1072-1080, 2011.

34. Tomasoni S, Longaretti L, Rota C, Morigi M, Conti S, Gotti E, Capelli C, Introna M, Remuzzi G, Benigni A: Transfer of growth factor receptor mRNA via exosomes unravels the regenerative effect of mesenchymal stem cells. *Stem Cells Dev.* 22: 772-780, 2013.

35. Lindoso RS, Collino F, Bruno S, Araujo DS, Sant'Anna JF, Tetta C, Provero P, Quesenberry PJ, Vieyra A, Einicker-Lamas M, Camussi G: Extracellular Vesicles Released from Mesenchymal Stromal Cells Modulate miRNA in Renal Tubular Cells and Inhibit ATP Depletion Injury. *Stem Cells* Dev., 2014. [Epub ahead of print].

36. Negishi K, Noiri E, Sugaya T, Li S, Megyesi J, Nagothu K, Portilla D: A role of liver fatty acid-binding protein in cisplatin-induced acute renal failure. *Kidney Int.* 72:348-358, 2007.

37. da Costa MR, Pizzatti L, Lindoso RS, Sant'Anna JF, DuRocher B, Abdelhay E, Vieyra A. Mechanisms of kidney repair by human mesenchymal stromal cells after ischemia: a comprehensive view using label-free MS(E). *Proteomics*.14:1480-1493, 2014.

38. Fang Y, Tian X, Bai S, Fan J, Hou W, Tong H, Li D. Autologous transplantation of adipose-derived mesenchymal stem cells ameliorates streptozotocin-induced diabetic nephropathy in rats by inhibiting oxidative stress, pro-inflammatory cytokines and the p38 MAPK signaling pathway. *Int J Mol Med.* 30:85-92, 2012.

39. Guo Y, Xiao L, Sun L, Liu F. Wnt/beta-catenin signaling: a promising new target for fibrosis diseases. *Physiol Res.* 17;61: 337-346, 2012.

40. Gonçalves JG, de Bragança AC, Canale D, Shimizu MH, Sanches TR, Moysés RM, Andrade L, Seguro AC, Volpini RA. Vitamin d deficiency aggravates chronic kidney disease progression after ischemic acute kidney injury. *PLoS One.* 9:e107228, 2014. doi: 10.1371/journal.pone.0107228.

41. Ying Y, Kim J, Westphal SN, Long KE, Padanilam BJ. Targeted Deletion of p53 in the Proximal Tubule Prevents Ischemic Renal Injury. *J Am Soc Nephrol*. 2014. pii: ASN.2013121270.

42. Oskowitz AZ, Penfornis P, Tucker A, Prockop DJ, Pochampally R. Drosha regulates hMSCs cell cycle progression through a miRNA independent mechanism. *Int J Biochem Cell Biol.* 43:1563-1572, 2011. doi: 10.1016/j.biocel.2011.07.005.

43. Aagaard L, Amarzguioui M, Sun G, Santos LC, Ehsani A, Prydz H, Rossi JJ. A facile lentiviral vector system for expression of doxycycline-inducible shRNAs: knockdown of the pre-miRNA processing enzyme Drosha. Mol Ther. 2007 May;15(5):938-45. Epub 2007 Feb 20. PubMed PMID: 17311008.

44. T Théry C, Ostrowski M, Segura E: Membrane vesicles as conveyors of immune responses. *Nat Rev Immunol.* 9:581-593, 2009. doi: 10.1038/nri2567.

45. Bruno S, Collino F, Deregibus MC, Grange C, Tetta C, Camussi G: Microvesicles derived from human bone marrow mesenchymal stem cells inhibit tumor growth. *Stem Cells Dev* 22:758-771. 2013. doi: 10.1089/scd.2012.0304.

46. Grange C, Tapparo M, Bruno S, Chatterjee D, Quesenberry PJ, Tetta C, Camussi G: Biodistribution of mesenchymal stem cell-derived extracellular vesicles in a model of acute kidney injury monitored by optical imaging. Int J Mol Med. 2014. 33: 1055-63.

47. Kim D, Pertea G, Trapnell C, Pimentel H, Kelley R, Salzberg SL: TopHat2: accurate alignment of transcriptomes in the presence of insertions, deletions and gene fusions. Genome Biol. 2013 14:R36.

48. Trapnell C, Hendrickson DG, Sauvageau M, Goff L, Rinn JL, Pachter L: Differential analysis of gene regulation at transcript resolution with RNA-seq. Nat Biotechnol. 2013, 31:46-53. doi: 10.1038/nbt.2450.

49. Huang da W, Sherman BT, Lempicki RA: Systematic and integrative analysis of large gene lists using DAVID bioinformatics resources. Nat Protoc. 2009, 4:44-57.

Figure legends

Figure 1. Characterization of MSC-Dsh cells. (A) FACS analysis of transduced wild type MSCs (MSC-CTRL, upper panel) and Drosha knock-down MSCs (MSC-Dsh, lower panel). Efficiency of transduction was measured as % of red fluorescence protein (RFP) positive cells. (B) Comparison of Drosha transcript expression in unsorted or RFP-sorted MSC-CTRL and MSC-Dsh measured by qRT-PCR. GAPDH transcript was used to normalize RNA input. (* $p<0.05$). Three different lines were tested. Data are mean ± SD of three different experiments.

Figure 2. Characterization of EV-Dsh surface markers and up-take by murine tubular epithelial cells (mTEC). **(**A) Representative FACS analyses of the expression of classical MSC markers (CD29, CD44, CD105, CD73, CD90 and HLA-class I) by EV-CTRL and EV-Dsh. Dot lines indicate the isotype controls. Three different EV preparations were tested with similar results. (B) Representative micrograph of incorporation of EV-CTRL and EV-Dsh by mTEC after 24 h of incubation. EVs were collected from MSC double-stained with Vybrant Dil (red) and SYTO-RNA (that labels the RNA, green). Original magnification X 200 and enlarged image X 630. Three experiments were performed with similar results.

Figure 3. Effect of intravenous injection of MSC-CTRL and MSC-Dsh in AKI mice. (A-C) Representative micrographs of renal histology of untreated AKI mice injected with PBS (A), and treated AKI injected with MSC-CTRL (B) or MSC-Dsh (C) cells (75.000 cells) and sacrificed at day 5 after glycerol administration. Original magnification, X 400 (D). Blood urea nitrogen (BUN, mg/dl) levels measured in healthy, untreated AKI and AKI mice treated with MSC-CTRL or MSC-Dsh, 5 days after glycerol administration. ANOVA with Newman–Keuls multicomparison test: * $p<0.05$ AKI and MSC-Dsh vs CTRL; ** $p<0.05$ MSC-CTRL vs MSC-Dsh. (E-F) Morphometric evaluation of hyalin casts (E) and tubular necrosis (F) in untreated AKI and AKI mice treated with MSC-CTRL or MSC-Dsh, 5 days after glycerol administration. Results are expressed as mean ± SEM (8 mice/group).

ANOVA with Newman–Keuls multicomparison test: *, $p<0.05$ MSC-CTRL vs AKI and ** , $p<0.05$ MSC-Dsh vs MSC-CTRL.

Figure 4. Effect of intravenous injection of EV-CTRL and EV-Dsh in AKI mice. (A-C) Representative micrographs of renal histology of untreated AKI (A) and AKI mice treated with EV-CTRL (B) or EV-Dsh (C) and sacrificed at day 5 after glycerol administration. Original magnification, X 400. (D-F) Representative micrographs of renal histology of untreated healthy (D) and healthy mice injected with EV-CTRL (E) or EV-Dsh (F) and sacrificed at day 2 after EV administration. (G) Blood urea nitrogen (BUN, mg/dl) levels measured in healthy, untreated AKI and AKI mice treated with EV-CTRL or EV-Dsh (5 healthy mice/group and 16 AKI mice/group). ANOVA with Newman–Keuls multicomparison test: * $p<0.05$ versus AKI; ** $p<0.05$ AKI EV-Dsh vs AKI EV-CTRL. (H-I) Morphometric evaluation of hyalin casts (H) and tubular necrosis (I) in untreated AKI and AKI-treated mice injected EV-CTRL or EV-Dsh 5 days after glycerol administration. Results are expressed as mean ± SEM; ANOVA with Newman–Keuls multicomparison test: *, $p<0.05$ EV-CTRL vs AKI and ** $p<0.05$, EV-Dsh vs EV-CTRL.

Figure 5. MSC-Dsh treatment induced in the kidney a different gene expression signature in respect to MSC-CTRL. (A) Pearson correlation of the global transcriptome profile of kidneys of healthy, untreated AKI and AKI treated with MSC-CTRL, MSC-Dsh, EV-CTRL and EV-Dsh. EV-CTRL and MSC-CTRL clustered into two major groups supporting an overlap in the genes regulated by both cells and EVs in AKI. Moreover, healthy mice significantly correlated with MSC-CTRL and EV-CTRL samples. On the contrary, transcriptomic profile of MSC-Dsh and EV-Dsh treated mice showed a high correlation with the untreated AKI mice. (B) Heatmap of the distribution of AKI-deregulated genes in –CTRL and –Dsh samples ($n=2663$, up AKI vs healthy; $n=1893$, down AKI vs healthy). (C) Median distribution of the fold changes in MSC- and EV-CTRL, MSC- and EV-Dsh in respect to AKI samples showing statistically different global distribution of all genes in the two groups.

Figure 6. Analysis of differentially expressed genes in MSC- or EV-CTRL treated mice versus AKI. (A, B) Venn diagram showing the number of genes up- or down-regulated (FC >= |1|) in the kidneys from AKI mice treated with MSC–CTRL and MSC-Dsh (A) or EV-CTRL and EV-Dsh (B) in respect to untreated AKI. (C, D) Venn diagram showing the number of genes commonly up- or down-regulated (C) in the kidneys from AKI mice treated with MSC- or EV-CTRL in respect to untreated AKI and (D) in the kidneys from AKI mice treated with MSC- or EV-CTRL in respect to AKI treated with MSC- or EV-Dsh. (E, F) Gene ontology analysis reveals that common modulated genes in AKI mice treated with MSC- or EV-CTRL, in respect to untreated AKI, are enriched (E) for genes associated with metabolic pathways, complement and coagulation cascades response (for the up-regulated) and (F) for genes associated with response to inflammation, ECM-receptor interaction, cell adhesion molecules and cell cycle (for the down-regulated).

Figure 7. Effect of wild type and Drosha-depleted MSC and EVs on markers of AKI. (A) Representative genomic occupancy profile of the Lcn2 gene among healthy, untreated AKI, MSC-treated (left panel) or EV-treated AKI (right panel). (B) qRT-PCR confirmation of Lcn2 modulation in mice after MSC- and EV- treatments in respect to untreated AKI mice (n=6 mice/group). Healthy mice are used as negative control. (C-D) Expression level of the three Fg subunits, detected by RNA-Seq analysis, among healthy, untreated AKI, MSC-treated (C) or EV-treated (D) AKI mice. (E) qRT-PCR confirmation of Fg-β expression in mice after MSC- and EV- treatments in respect to untreated AKI mice (n=6 mice/group). In healthy mice no or minimal expression of all the Fg-subunits was observed. (F) Immunohistochemistry analysis of Fg-β among healthy, untreated AKI, MSC- and EV- treated animals. Tubular staining was not observed in kidneys from healthy mice and was markedly reduced in mice treated with MSC- and EV-CTRL but not in MSC and EV–Dsh injected mice. AKI untreated, MSC- and EV-Dsh treated animals showed a strong peritubular and some cytoplasmic tubular staining.

For qRT-PCR analysis, data are expressed as mean ± SD; ANOVA with Newman–Keuls multicomparison test: * $p<0.05$ vs AKI and ** $p<0.05$ vs –CTRL.

Table 1. miRNAs down-regulated in EV-Dsh in respect to EV-CTRL**.** The relative expression of miRNAs in EV-Dsh was defined as fold change evaluated as $2^{-\Delta\Delta Ct}$ in respect to the reference sample (EV-CTRL) as described in Materials and Methods (n=4/each group, $p < 0,05$).

Target Name	Rq mean	SD	T test	Target Name	Rq mean	SD	T test
hsa-miR-215	*0,04*	*0,04*	*2,27E-05*	**hsa-miR-483-5p**	*0,28*	*0,28*	*0,014658*
hsa-miR-28-3p	*0,28*	*0,08*	*0,000415*	**hsa-miR-106a**	*0,50*	*0,20*	*0,015468*
hsa-miR-376a	*0,43*	*0,09*	*0,001068*	**hsa-miR-590-5p**	*0,30*	*0,29*	*0,017129*
hsa-miR-24	*0,67*	*0,06*	*0,001268*	**hsa-miR-376c**	*0,57*	*0,18*	*0,017469*
hsa-miR-1227	*0,23*	*0,13*	*0,001392*	**hsa-miR-133a**	*0,47*	*0,22*	*0,018088*
hsa-miR-30e-3p	*0,53*	*0,09*	*0,001867*	**hsa-miR-423-5p**	*0,22*	*0,19*	*0,018506*
hsa-miR-411	*0,45*	*0,11*	*0,002006*	**hsa-miR-425-5p**	*0,46*	*0,24*	*0,020084*
mmu-miR-129-3p	*0,13*	*0,18*	*0,002474*	**hsa-miR-29a**	*0,67*	*0,15*	*0,022468*
hsa-miR-486	*0,22*	*0,17*	*0,00274*	**hsa-miR-574-3p**	*0,57*	*0,20*	*0,024011*
hsa-miR-218	*0,33*	*0,15*	*0,002831*	**hsa-let-7d**	*0,59*	*0,19*	*0,024324*
hsa-miR-889	*0,22*	*0,17*	*0,002908*	**hsa-miR-150**	*0,64*	*0,18*	*0,026056*
hsa-miR-1243	*0,19*	*0,19*	*0,003278*	**hsa-miR-19b**	*0,62*	*0,19*	*0,029332*
hsa-miR-345	*0,38*	*0,15*	*0,003789*	**hsa-miR-33a#**	*0,24*	*0,40*	*0,031748*
mmu-miR-140	*0,50*	*0,13*	*0,004866*	**hsa-miR-1208**	*0,54*	*0,24*	*0,032548*
hsa-miR-186	*0,34*	*0,19*	*0,005884*	**hsa-miR-191**	*0,63*	*0,20*	*0,033122*
hsa-miR-382	*0,22*	*0,22*	*0,00613*	**hsa-miR-203**	*0,58*	*0,23*	*0,035758*
hsa-miR-146b	*0,55*	*0,13*	*0,006271*	**hsa-miR-200c**	*0,40*	*0,34*	*0,03695*
hsa-miR-202	*0,18*	*0,24*	*0,006639*	**hsa-miR-181a**	*0,55*	*0,25*	*0,038543*

hsa-miR-10a	*0,28*	*0,22*	*0,007002*	**hsa-miR-487b**	*0,43*	*0,32*	*0,03889*
hsa-miR-323-3p	*0,27*	*0,22*	*0,007399*	**hsa-miR-17**	*0,63*	*0,21*	*0,04191*
hsa-miR-214	*0,49*	*0,16*	*0,007832*	**hsa-miR-532**	*0,54*	*0,27*	*0,04398*
hsa-miR-744	*0,45*	*0,18*	*0,008342*	**hsa-miR-148a**	*0,34*	*0,25*	*0,044801*
mmu-miR-134	*0,39*	*0,20*	*0,008937*	**hsa-miR-328**	*0,48*	*0,31*	*0,044856*
hsa-miR-199a	*0,27*	*0,25*	*0,00985*	**hsa-miR-29c**	*0,56*	*0,28*	*0,049784*
hsa-let-7b	*0,60*	*0,15*	*0,01334*				

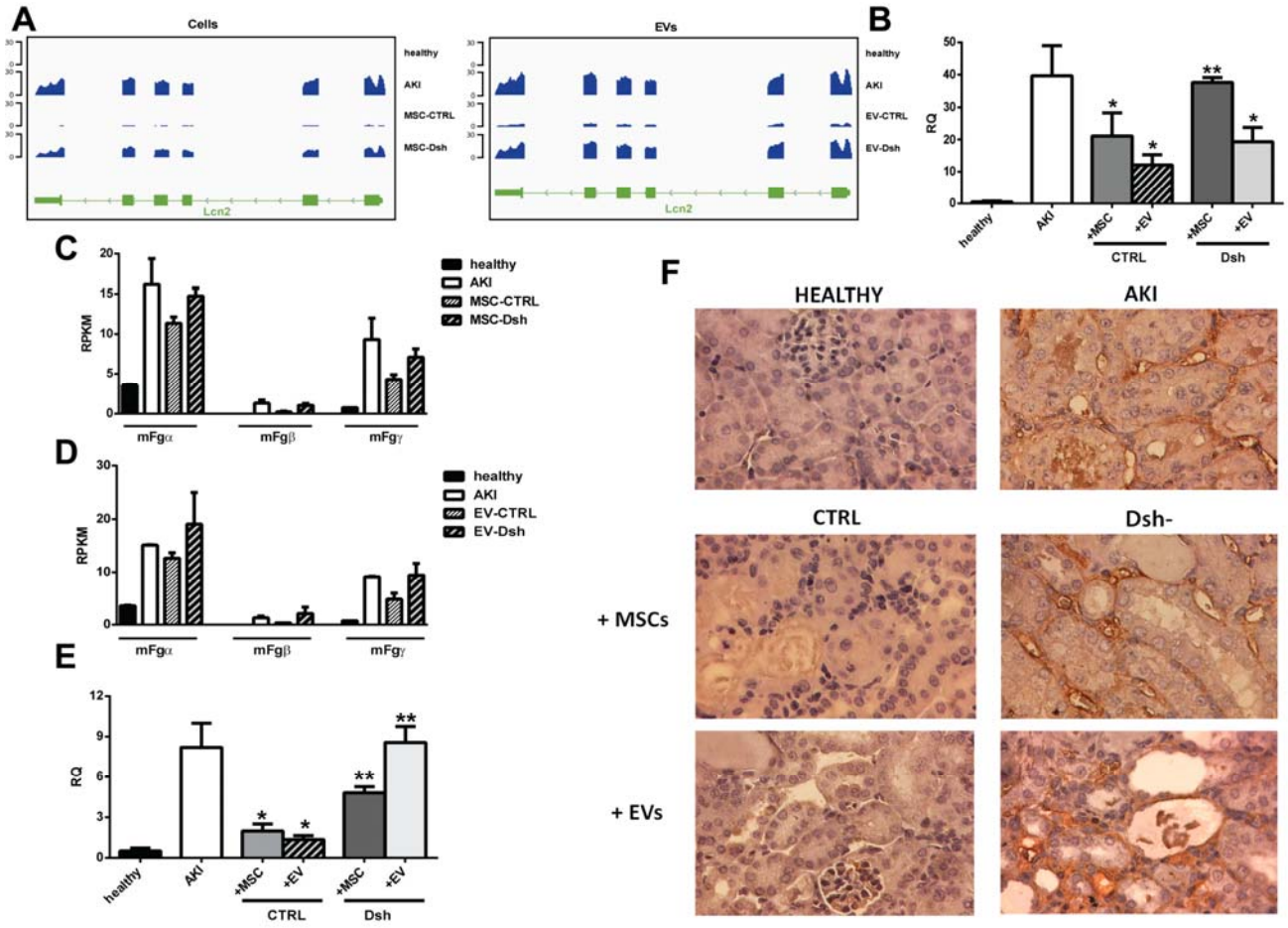
A
Cells
EVs
healthy
AKI
MSC-CTRL
MSC-Dsh
EV-CTRL
EV-Dsh
Lcn2
B
RQ
healthy
AKI
+MSC
+EV
CTRL
Dsh
C
RPKM
mFgα
mFgβ
mFgγ
D
E
F
HEALTHY
AKI
CTRL
Dsh-
+ MSCs
+ EVs

Figure 7

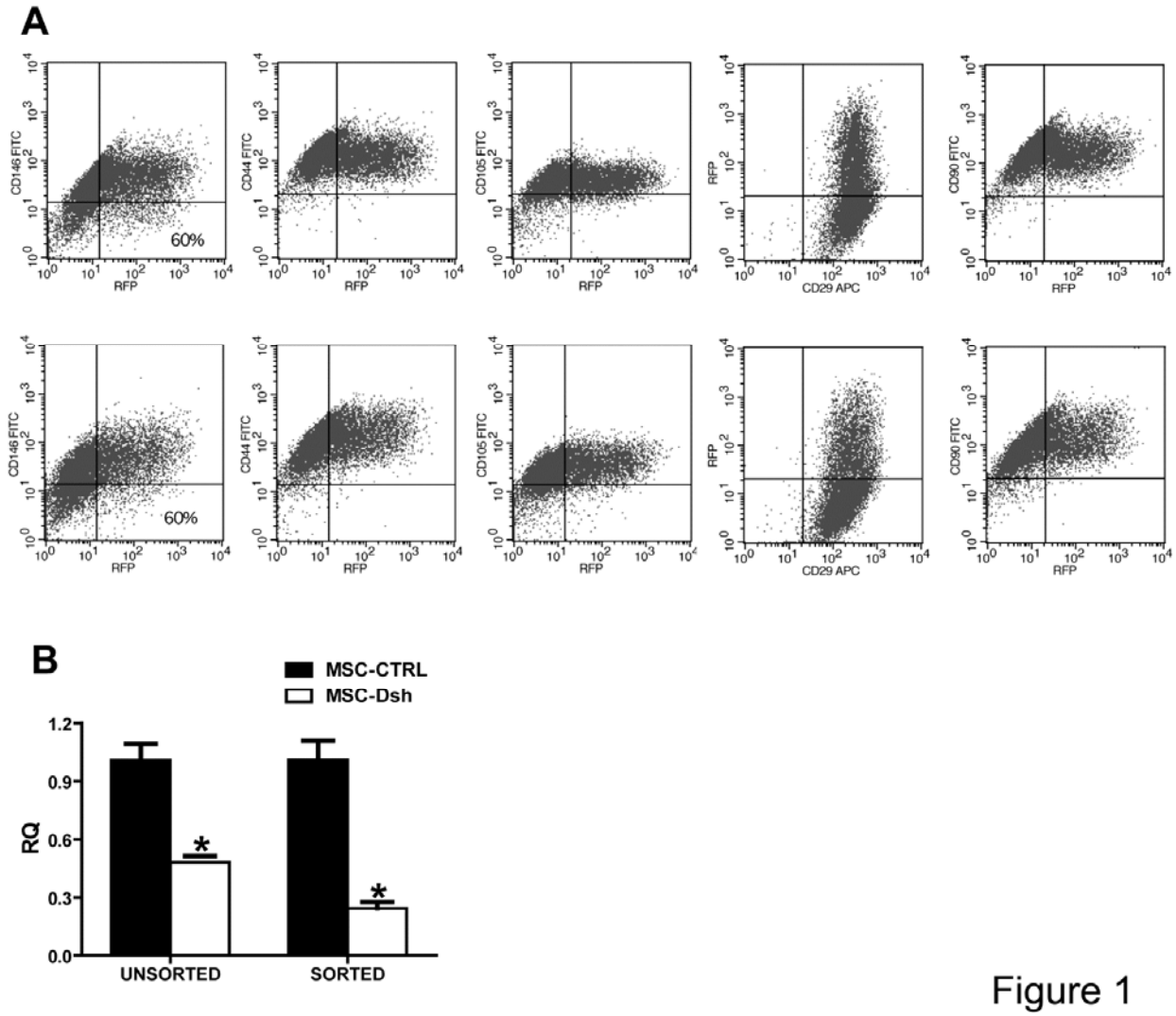
A
CD146 FITC
CD44 FITC
CD105 FITC
RFP
CD90 FITC
CD29 APC
60%
60%
RFP
B
MSC-CTRL
MSC-Dsh
RQ
1.2
0.9
0.6
0.3
0.0
*
*
UNSORTED
SORTED

Figure 1

1

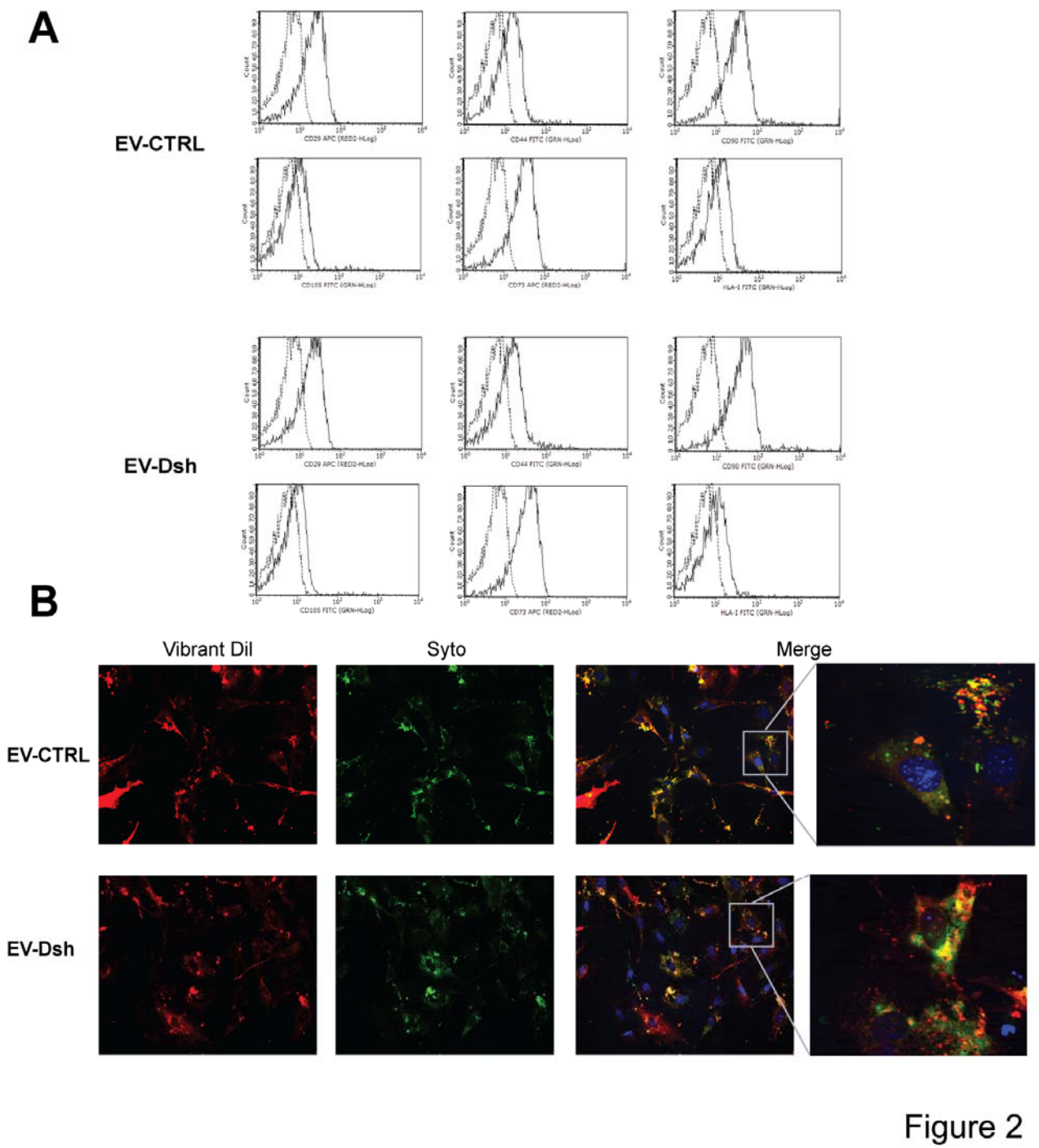
A
EV-CTRL
EV-Dsh
CD29 APC (RED2-HLog)
CD44 FITC (GRN-HLog)
CD90 FITC (GRN-HLog)
CD105 FITC (GRN-HLog)
CD73 APC (RED2-HLog)
HLA-1 FITC (GRN-HLog)
B
Vibrant DiI
Syto
Merge
EV-CTRL
EV-Dsh

Figure 2

1

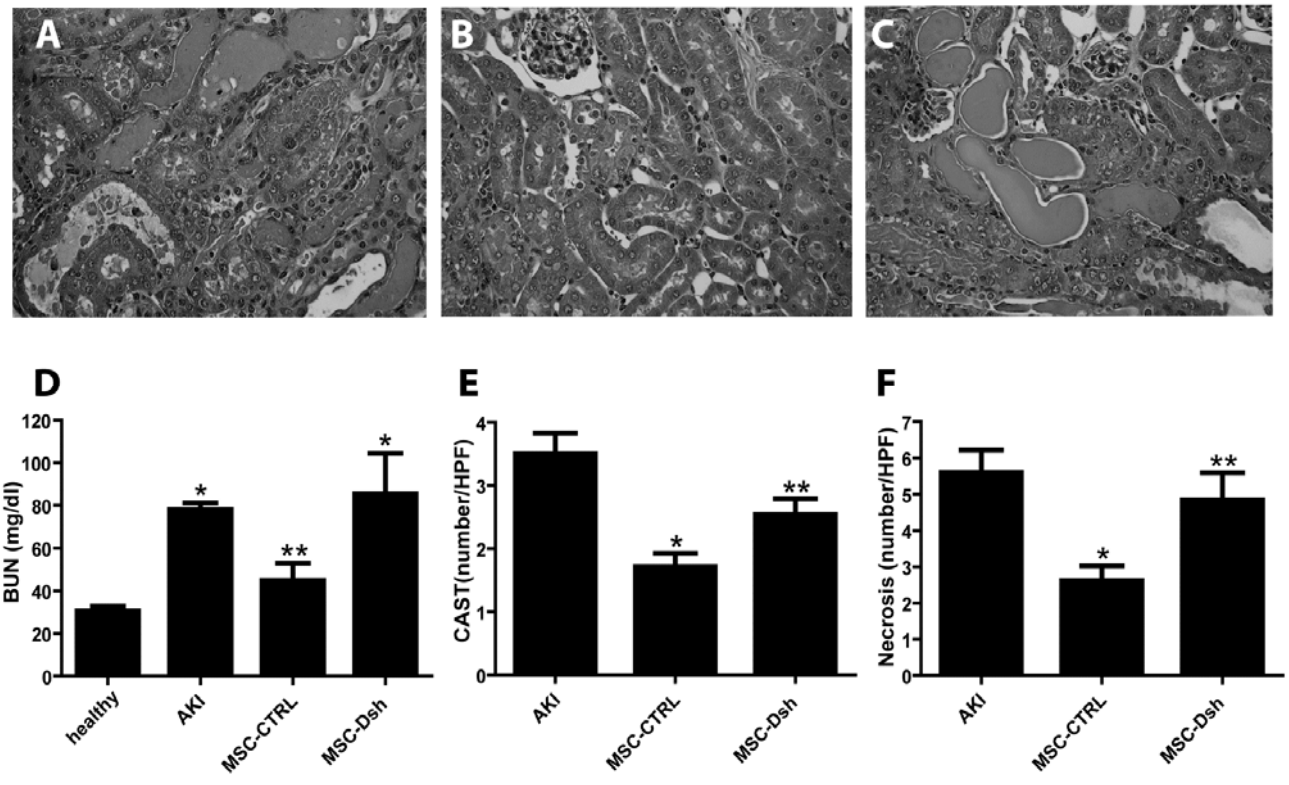
A
B
C
D
BUN (mg/dl)
120
100
80
60
40
20
0
*
**
*
healthy
AKI
MSC-CTRL
MSC-Dsh
E
CAST(number/HPF)
4
3
2
1
0
*
**
AKI
MSC-CTRL
MSC-Dsh
F
Necrosis (number/HPF)
7
6
5
4
3
2
1
0
*
**
AKI
MSC-CTRL
MSC-Dsh

1

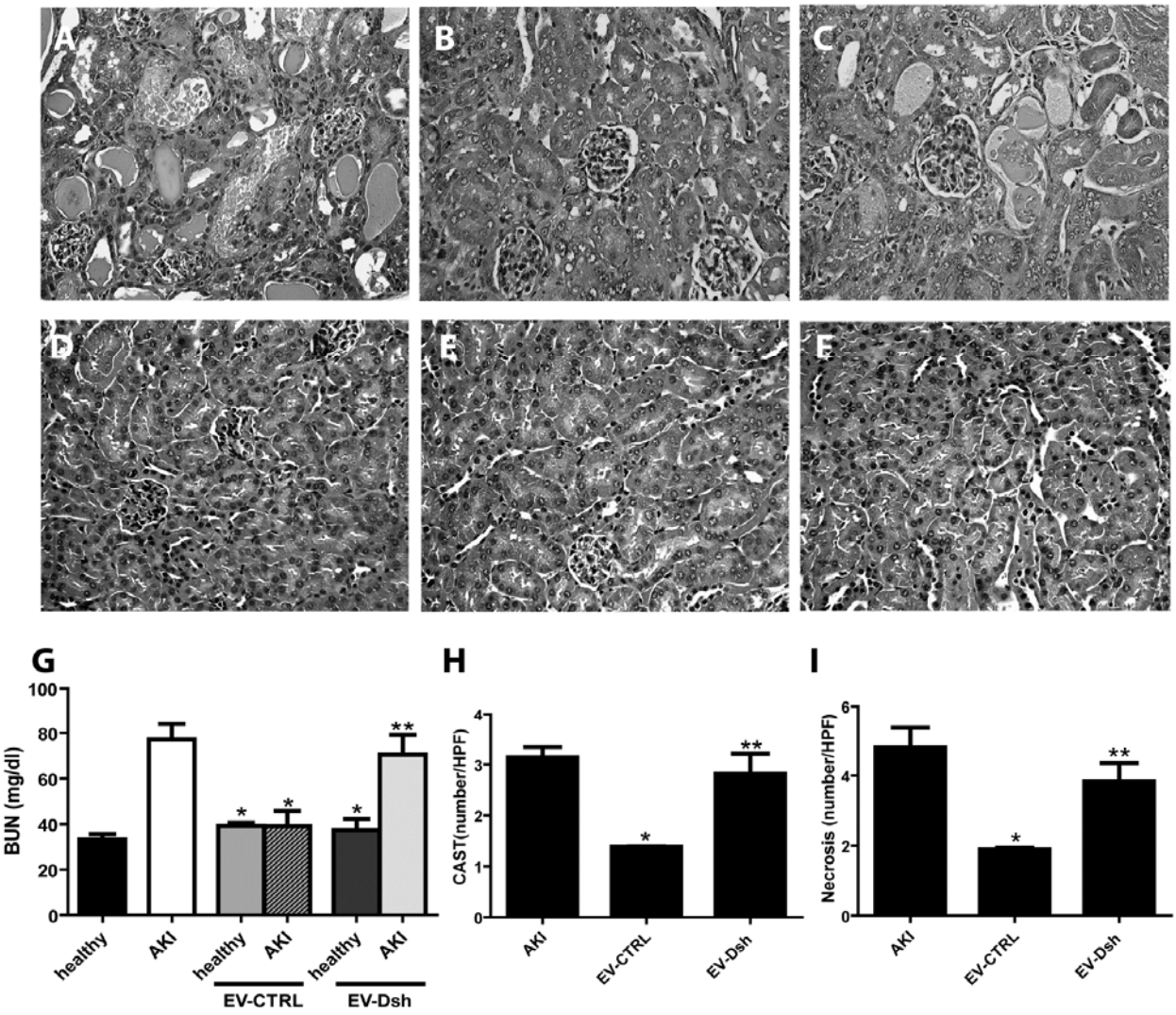
A
B
C
D
E
F
G
BUN (mg/dl)
100
80
60
40
20
0
healthy
AKI
healthy
AKI
healthy
AKI
EV-CTRL
EV-Dsh
H
CAST(number/HPF)
4
3
2
1
0
AKI
EV-CTRL
EV-Dsh
I
Necrosis (number/HPF)
6
4
2
0
AKI
EV-CTRL
EV-Dsh

Figure 4

1

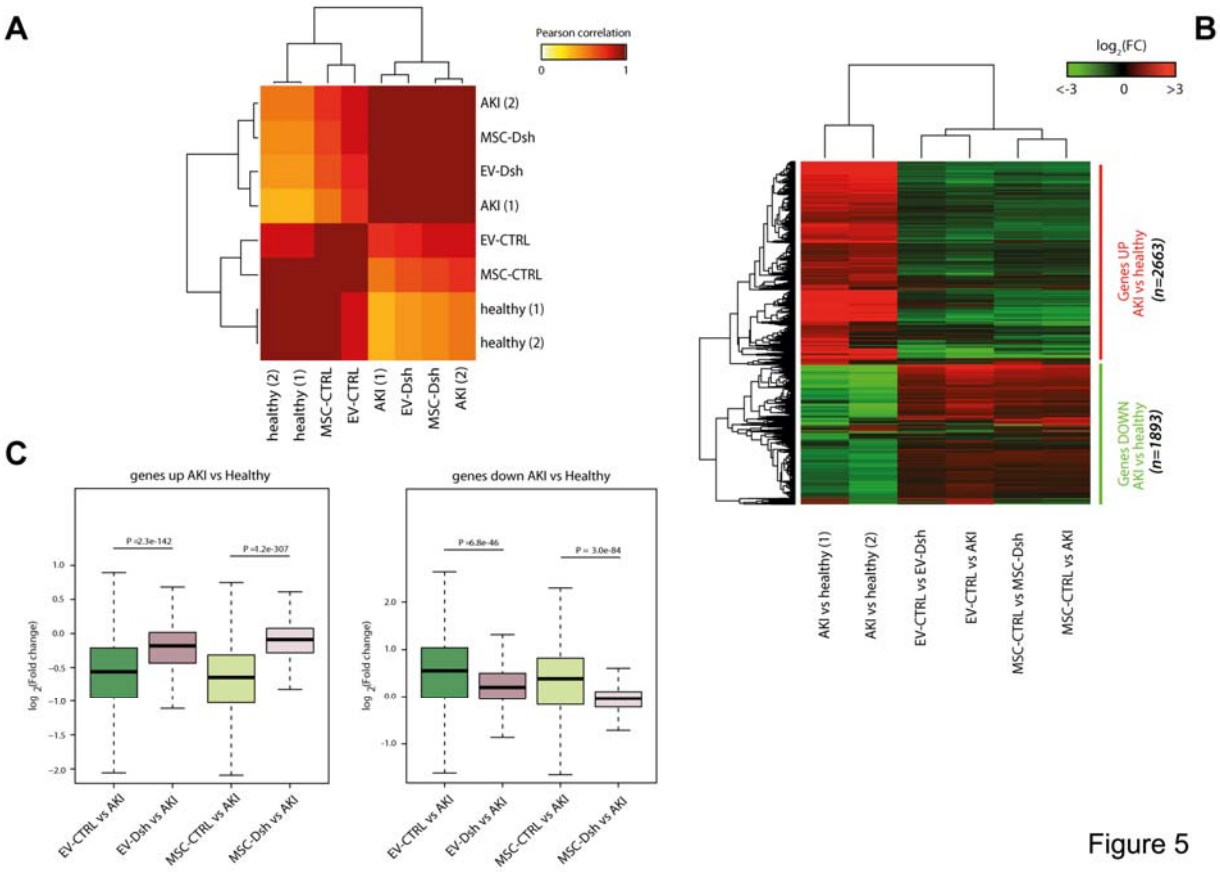
A
Pearson correlation
0
1
AKI (2)
MSC-Dsh
EV-Dsh
AKI (1)
EV-CTRL
MSC-CTRL
healthy (1)
healthy (2)
healthy (2)
healthy (1)
MSC-CTRL
EV-CTRL
AKI (1)
EV-Dsh
MSC-Dsh
AKI (2)
B
log2(FC)
<-3
0
>3
Genes UP
AKI vs healthy
(n=2663)
Genes DOWN
AKI vs healthy
(n=1893)
AKI vs healthy (1)
AKI vs healthy (2)
EV-CTRL vs EV-Dsh
EV-CTRL vs AKI
MSC-CTRL vs MSC-Dsh
MSC-CTRL vs AKI
C
genes up AKI vs Healthy
P =2.3e-142
P =1.2e-307
log 2(Fold change)
EV-CTRL vs AKI
EV-Dsh vs AKI
MSC-CTRL vs AKI
MSC-Dsh vs AKI
genes down AKI vs Healthy
P =6.8e-46
P = 3.0e-84
log 2(Fold change)
EV-CTRL vs AKI
EV-Dsh vs AKI
MSC-CTRL vs AKI
MSC-Dsh vs AKI

Figure 5

1

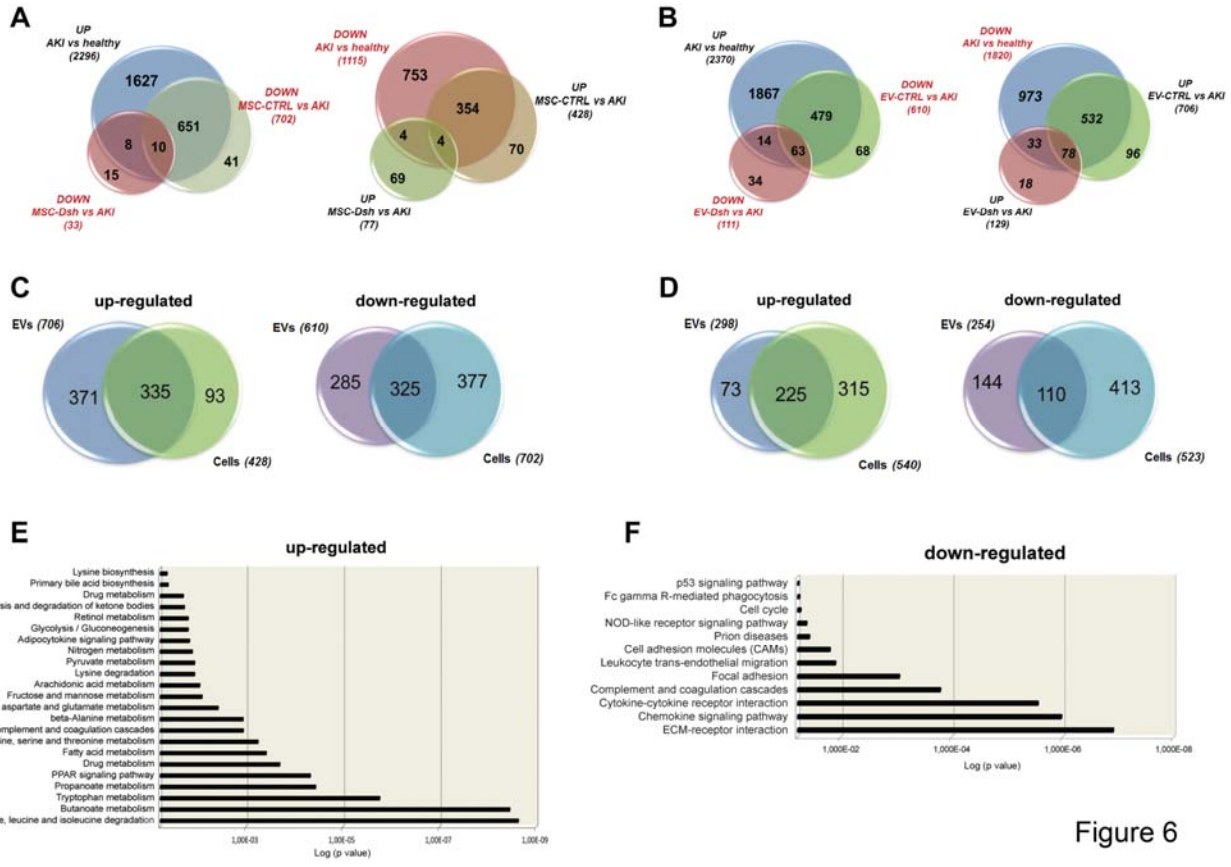
A
UP
AKI vs healthy
(2296)
1627
651
8
10
41
15
DOWN
MSC-CTRL vs AKI
(702)
DOWN
MSC-Dsh vs AKI
(33)
DOWN
AKI vs healthy
(1115)
753
354
4
4
70
69
UP
MSC-CTRL vs AKI
(428)
UP
MSC-Dsh vs AKI
(77)
B
UP
AKI vs healthy
(2370)
1867
479
14
63
68
34
DOWN
EV-CTRL vs AKI
(610)
DOWN
EV-Dsh vs AKI
(111)
DOWN
AKI vs healthy
(1820)
973
532
33
78
96
18
UP
EV-CTRL vs AKI
(706)
UP
EV-Dsh vs AKI
(129)
C
up-regulated
EVs (706)
371
335
93
Cells (428)
down-regulated
EVs (610)
285
325
377
Cells (702)
D
up-regulated
EVs (298)
73
225
315
Cells (540)
down-regulated
EVs (254)
144
110
413
Cells (523)

E
up-regulated
Lysine biosynthesis
Primary bile acid biosynthesis
Drug metabolism
Synthesis and degradation of ketone bodies
Retinol metabolism
Glycolysis / Gluconeogenesis
Adipocytokine signaling pathway
Nitrogen metabolism
Pyruvate metabolism
Lysine degradation
Arachidonic acid metabolism
Fructose and mannose metabolism
Alanine, aspartate and glutamate metabolism
beta-Alanine metabolism
Complement and coagulation cascades
Glycine, serine and threonine metabolism
Fatty acid metabolism
Drug metabolism
PPAR signaling pathway
Propanoate metabolism
Tryptophan metabolism
Butanoate metabolism
Valine, leucine and isoleucine degradation
1,00E-03
1,00E-05
1,00E-07
1,00E-09
Log (p value)

F
down-regulated
p53 signaling pathway
Fc gamma R-mediated phagocytosis
Cell cycle
NOD-like receptor signaling pathway
Prion diseases
Cell adhesion molecules (CAMs)
Leukocyte trans-endothelial migration
Focal adhesion
Complement and coagulation cascades
Cytokine-cytokine receptor interaction
Chemokine signaling pathway
ECM-receptor interaction
1,000E-02
1,000E-04
1,000E-06
1,000E-08
Log (p value)

Figure 6

1